Available online at www.sciencedirect.com
SCIENCE DIRECT®
Journal of Nuclear Materials 344 (2005) 198–205
journal of nuclear materials
www.elsevier.com/locate/jnucmat

Modelling thermal properties of actinide dioxide fuels

V. Sobolev *

SCK·CEN, Belgian Nuclear Research Centre, Boeretang 200, B-2400 Mol, Belgium

Abstract

Modelling of the behaviour of fuels and targets containing minor actinides is still difficult because of very limited information on their thermal and mechanical properties. Integral analysis based on the sound physical models and on the similarity principle can be very useful in this situation. In the current article, a combination of macroscopic and microscopic approaches is used for development of an equation of state (EOS) for actinide dioxide fuels. Based on simple but physically complete models of phonon and electron spectra, the EOS was deduced in quasi-harmonic approximation, and useful relationships bounding thermal and mechanical properties were obtained. They were firstly tested with calculation of the specific heat and the coefficient of thermal expansion of UO_2 and ThO_2. A good agreement with the experimental data was demonstrated in the temperature range of 30–1600 K. Then the model was successfully applied to NpO_2 and PuO_2. Lack of experimental data on thermal properties of AmO_2 and CmO_2 in open literature did not allow the reliable comparison.

1. Introduction

Modelling of thermal and mechanical properties of actinide oxide fuels with a high concentration of plutonium (Pu) and minor actinides (MA) is a problem of considerable importance in the design of new generation reactors devoted to their burning. In literature this kind of data are very scarce and often show a wide spread because of the difficulties related to their production and properties measurement. Few sophisticated techniques have been used for estimation of the thermomechanical properties of UO_2, ThO_2 and MOX: molecular dynamics was used by Basak et al. [1], Kurosaki et al. [2] and Lindan and Cillanet [3], Dolling et al. [4] used the lattice dynamic approach and the shell model. These techniques, however, are difficult and the obtained results can not be directly implemented in the fuel performance codes. In many cases a combined simplified physical modelling and the similarity principle allow to deduce the missing data basing on the data of the well known materials. The merit of this approach is the basic understanding and a possibility to extrapolate the data out of the range of measurements.

This article presents the first results obtained with this approach for some actinide dioxides of interest: ThO_2, NpO_2, UO_2, PuO_2, AmO_2, and CmO_2. In the next chapter, a brief reminder is given about the equation of state (EOS) and its use for calculation of the thermodynamic properties of solids. The third chapter describes the approaches used for construction of the AnO_2 EOS. Then the obtained EOS is used for deduction of the relationships for specific heat and coefficient of thermal expansion. At the end, the results of the model validation by predicting the properties of UO_2 and ThO_2

* Tel.: +32 14 33 22 67; fax: +32 14 32 15 29.
E-mail address: vsobolev@sckcen.be

0022-3115/$ - see front matter © 2005 Elsevier B.V. All rights reserved.
doi:10.1016/j.jnucmat.2005.04.042

and its application to PuO_2, NpO_2, AmO_2 and CmO_2 are discussed and compared with the available data.

2. Equation of state and relations between thermal and mechanical parameters

Once EOS is known for a solid, one can determine its various thermodynamic (TD) properties at equilibrium. Two types of EOS are mostly used – caloric and thermal. The first expresses one of TD potentials (e.g. the Helmholtz free energy F) through the TD variables (pressure p, volume V, temperature T, ...): $F = F(V, T)$, the second bounds the TD variables themselves: $p = p(V, T)$. These two types of EOS are interrelated

$$p(V,T) = -\left(\frac{\partial F(V,T)}{\partial V}\right)_T \tag{1}$$

and determine the main TD parameters of a solid: the isobaric coefficient of thermal expansion (CTE) $\alpha_p \equiv \frac{1}{V}\left(\frac{\partial V}{\partial T}\right)_p$, the isothermal bulk modulus $B_T \equiv -V\left(\frac{\partial p}{\partial V}\right)_T$, the isochoric heat capacity $C_V = -T\left(\frac{\partial^2 F}{\partial T^2}\right)_V$, the isobaric heat capacity $C_p = C_V + \alpha_p^2 \cdot B_T \cdot V \cdot T$.

One of the most recognised theoretical approaches used for the EOS deduction is the microscopic statistical approach, which considers a solid as a 'special box' filled with a gas of quasi-particles related to atom vibrations (phonons) and to electronic excitations. The Helmholtz free energy (caloric EOS) of this system is a sum of the solid static energy, the phonon free energy and the contribution of all types of the electronic excitations:

$$F(V,T) = E_{0\,st}(V) + F_{\mathrm{ph}}(V,T) + F_{\mathrm{el}}(V,T). \tag{2}$$

In the quasi-harmonic approximation, the phonon free energy of the ideal solid with the volume V can be presented as follows [5]:

$$F_{\mathrm{ph}}(V,T) = E_{\mathrm{ph}\,0}(V) + 3N_{at}\cdot k_{\mathrm{B}}T \cdot \sum_i \int_0^{\omega_{\max}} \ln\left(1 - \mathrm{e}^{-\frac{\hbar\cdot\omega(V)}{k_B T}}\right)\cdot f_i(\omega(V))\,\mathrm{d}\omega, \tag{3}$$

where i is the index of the phonon branch; ω the phonon angular frequency; $f(\omega)$ the phonon spectrum; $\hbar$ the Planck's constant; k_{B} the Boltzmann constant and $E_{\mathrm{ph}0}$ the energy of the lattice vibrations at $T = 0$ given by the expression:

$$E_{0\,\mathrm{ph}}(V) = \frac{3N_{at}\cdot\hbar}{2}\cdot\sum_i \omega_{0i}(V). \tag{4}$$

At $T < 2000$ K the electronic component of free energy will mainly be determined by the excitations of the unpaired localised electrons [6]:

$$F_{\mathrm{el}}(V,T) = E_{0\,\mathrm{el}}(V) - k_{\mathrm{B}}T\cdot\ln\sum_j g_j\cdot\mathrm{e}^{\frac{-\varepsilon_{ej}(V)}{k_{\mathrm{B}}\cdot T}}, \tag{5}$$

where ε_{ej} is the electron energy at the jth level; g_j the degeneracy of the jth level; $E_{0\,\mathrm{el}}(V) \approx const$-energy of the ground state level which can be assumed to be zero for the excitations.

The static energy of the lattice can be deduced from the well known EOS of Kumar [7], assuming that in the considered region of temperature and pressure $(V - V_0)/V_0 \ll 1$:

$$E_{0st}(V) \approx \frac{B_{T_0}\cdot(V - V_0)^2}{V_0}. \tag{6}$$

The thermal EOS can be obtained from the caloric EOC (2) by using Eq. (1):

$$p(V,T) = -\frac{2B_{To}\cdot(V - V_0)}{V_0} + \frac{3N_{at}\cdot\hbar}{V}\sum_i \gamma_{Gi} \cdot\left(\frac{\omega_{i0}}{2} + \langle\omega\rangle_i\right) + N_{at}\left\langle\frac{\partial\varepsilon_j}{\partial V}\right\rangle, \tag{7}$$

where $\gamma_{Gi} \equiv -\frac{\partial(\ln\langle\omega_i\rangle)}{\partial(\ln V)}$ is the Grunëisen parameter for the ith phonon branch; $\langle\omega\rangle_i = \int_0^{\omega_{\max}} \frac{\omega(V)\cdot f_i(\omega)\,\mathrm{d}\omega}{\exp(\hbar\cdot\omega(V)/k_B T) - 1}$ -average phonon frequency in the ith branch; $\left\langle\frac{\partial\varepsilon_{ej}}{\partial V}\right\rangle = \frac{\sum_j g_j\cdot\mathrm{e}^{-\varepsilon_{ej}/k_B T}\cdot\frac{\partial\varepsilon_{ej}}{\partial V}}{\sum_j g_j\cdot\mathrm{e}^{-\varepsilon_{ej}/k_B T}}$.

Eq. (7) can be considered as a generalised quasi-harmonic Grunëisen EOS where anharmonic interactions are taken into account through dependence of the phonon frequencies upon the volume. The spectra of phonons and electronic excitations have to be determined for the considered system.

3. Phonon spectrum model

Some simplified models of the solid phonon spectrum are used in practice. The most known is the Debye model which considers a solid as non-dispersive elastic continuum with the linear relationship between the phonon frequency and the wave vector. The optical modes are neglected in this model, therefore its application to the solids with more than one atom in the primitive cell can lead to incorrect results. The most simple possibility to take into account the optical phonons is to describe them with the Einstein model, which postulates that the vibrations of all atoms have the same frequency [5,8]. However, this is very far from the reality and can produce erroneous conclusions for solids with a complex primitive cell.

AnO_2 has the fluorite type crystal structure with the polyhedral primitive cell containing three complete atoms – one An and two O (Fig. 1). Therefore its phonon spectrum consists of nine branches: three acoustic translational vibrations (one with the longitudinal polarisation – LA, and two identical branches with the transverse polarisation-2 × TA) and six optical branches,

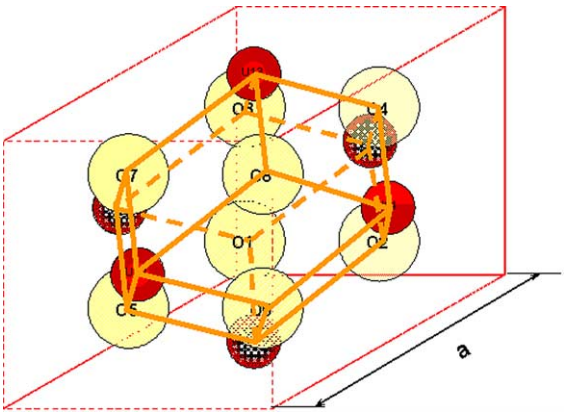

Fig. 1. Primitive cell of AnO_2 crystal.

describing the atoms vibrations within the cell (two doubly degenerated transverse: $2\times TO_1$, $2\times TO_1$, and two different longitudinal: LO_1, LO_2) [4]. In order to construct a simple spectrum model, the first Brilluen zone (BZ) corresponding to the primitive cell above was approximated by the sphere with a diameter of $2\pi/a'$, where a' is the distance between two neighbour A_n atoms in the primitive cell. Then the spectrum of the acoustic branches was described with the Debye functions, and that of the optical branches-with the stepwise functions. The maximum frequencies for the acoustic branches were found from the dispersion relations, taking into account the Bragg's limitation on the maximum wave vector:

$$\omega_{Ai} = k_{\max}\cdot v_i = \frac{\pi\cdot v_i}{a'} \quad (i=1,2,3), \tag{8}$$

where v_i is the velocity of sound with the polarization i. Taking into account the details of the UO_2 phonon spectrum obtained in [4] (see Fig. 2), we proposed a simplified optical phonon spectrum containing only two branches: one doubly degenerated longitudinal and one quadruple degenerated transverse. In order to fix the limiting frequencies $\omega_{i\min}$ and $\omega_{i\max}$, the following assumptions were made:

- two longitudinal optic branches were presented as a large stepwise doubly degenerated branch ($LO_1 + LO_2 \rightarrow 2\times LO$ with the lowest frequency equal to the highest frequency of the longitudinal acoustic branch and with three times greater the highest frequency;
- doubly degenerated transverse optic branches were presented by a large stepwise quadruple degenerated branch ($2\times TO_1 + 2\ \times TO_2 \rightarrow 4\times TO$ with the same lowest frequency as that of the longitudinal optic branch and with the highest frequency determined by the Lyddane's relationship [4].

Using the assumptions above, one can present the AnO_2 phonon spectrum model as follows:

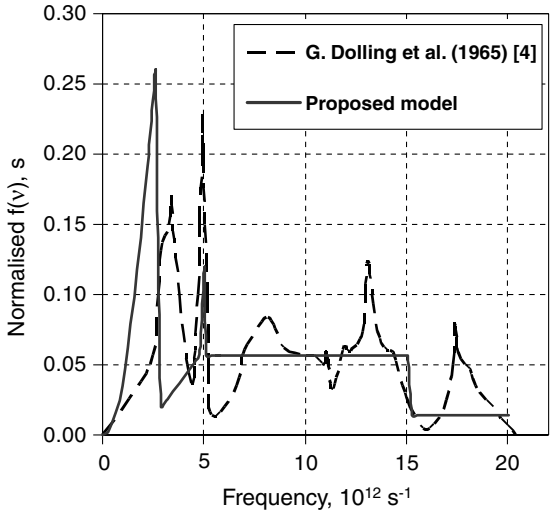

Fig. 2. The proposed simple model of UO_2 phonon spectrum (a) and the phonon spectrum obtained with the shell model (b) in Ref. [4].

$$\begin{aligned} f_{\rm ph}(\omega) = {} & \frac{\omega^2\cdot \mathrm{Sign}(\omega_{LA}-\omega)}{3\omega_{LA}^3} + \frac{2\omega^2\cdot \mathrm{Sign}(\omega_{TA}-\omega)}{3\omega_{TA}^3} \\ & + \frac{4}{9}\cdot\frac{\mathrm{Sign}(\omega-\omega_{TO\min}) - \mathrm{Sign}(\omega-\omega_{TO\max})}{(\omega_{TO\max}-\omega_{TO\min})} \\ & + \frac{2}{9}\cdot\frac{\mathrm{Sign}(\omega-\omega_{LO\min}) - \mathrm{Sign}(\omega-\omega_{LO\max})}{(\omega_{LO\max}-\omega_{LO\min})}. \end{aligned} \tag{9}$$

Comparison of this model with the spectrum obtained by Dolling shows that it reflects rather satisfactory the main features of the UO_2 spectrum (Fig. 2).

4. Free energy, heat capacity and linear thermal expansion of AnO_2 system

The phonon spectrum (9) allows to deduce the following caloric EOS for AnO_2 system:

$$\begin{aligned} & F(V,T) \\ & = \frac{B_{To}\cdot(V-V_0)^2}{V_0} + \frac{3N_{at}k_{\rm B}}{2}\cdot\left[\frac{\theta_{AL}(V)}{12} + \frac{\theta_{AT}(V)}{6}\right. \\ & \left. + \frac{\theta_{OL\max}(V)-\theta_{OL\min}(V)}{9} + \frac{2\cdot(\theta_{OL\max}(V)-\theta_{OL\min}(V))}{9}\right] \\ & + 3N_{at}\cdot k_{\rm B}T\cdot\left\{\frac{1}{3}\ln\left(1-e^{-\frac{\theta_{AL}(V)}{T}}\right) - \frac{1}{9}D_3(\theta_{AL}(V)/T)\right. \\ & + \frac{2}{3}\ln\left(1-e^{-\frac{\theta_{AT}(V)}{T}}\right) - \frac{2}{9}D_3(\theta_{AT}(V)/T) \\ & + \frac{2}{3}\ln\left(1-e^{-\frac{\theta_{OL\max}(V)-\theta_{OL\min}(V)}{T}}\right) - \frac{2}{9} \\ & \cdot\frac{\theta_{OL\max}(V)\cdot D_1(\theta_{OL\max}(V)/T) - \theta_{OL\min}(V)\cdot D_1(\theta_{OL\min}(V)/T)}{\theta_{OL\max}(V)-\theta_{OL\min}(V)} \\ & + \frac{4}{3}\ln\left(1-e^{-\frac{\theta_{OT\max}(V)-\theta_{OT\min}(V)}{T}}\right) \\ & - \frac{4}{9}\cdot\frac{\theta_{OT\max}(V)\cdot D_1(\theta_{OT\max}(V)/T) - \theta_{OT\min}(V)\cdot D_1(\theta_{OT\min}(V)/T)}{\theta_{OT\max}(V)-\theta_{OT\min}(V)} \\ & \left. - \frac{1}{9}\ln\left(\sum_j g_j\cdot e^{-\frac{\theta_{cj}(V)}{T}}\right)\right\}, \end{aligned} \tag{10}$$

where

$$\theta_{\mathrm{ph}\,i} \equiv \frac{\hbar \cdot \omega_i}{k_\mathrm{B}}, \quad \theta_{ej} = \frac{\varepsilon_{ej}}{k_\mathrm{B}},$$

phonon and electron characteristic temperatures, and

$$D_n(y) = \frac{n}{y^n} \cdot \int_0^y \frac{x^n \,\mathrm{d}x}{\exp(x) - 1},$$

the first kind Debye integrals of the nth order.

Two first terms of (10) describe the ground state energy, the last term is the electronic excitation component, and all other describe the contribution of acoustic and optic phonons to TD potential. The thermal EOS can be deduced from (10) by using (1):

$$p(V,T) = -\frac{\partial E_0}{\partial V} + \frac{3N_{at} \cdot T}{V} \cdot \left[\frac{1}{3}\sum_{i=1}^{3}\gamma_{Gi} \cdot D_3'(\theta_i/T) + \frac{1}{9}\sum_{i=4}^{9}\gamma_{Gi} \cdot \frac{\theta_{i\max} \cdot D_1'(\theta_{i\max}/T) - \theta_{i\min} \cdot D_1'(\theta_{i\min}/T)}{\theta_{i\max} - \theta_{i\min}}\right] + \left\langle \frac{\partial \varepsilon_{ej}}{\partial V} \right\rangle, \tag{11}$$

where

$$D_n'(y) = \frac{n}{y^n} \cdot \int_0^y \frac{x^{n+1} \cdot \exp(x) \cdot \mathrm{d}x}{(\exp(x) - 1)^2},$$

the second kind Debye integral of the nth order.

The isochoric heat capacity can be obtained by the double differentiation of (10):

$$C_V = 3k_\mathrm{B}N_{at} \cdot \left[\frac{1}{3} \cdot \sum_{i=1}^{3} D_3'(\theta_i/T) + \frac{1}{9} \cdot \sum_{i=4}^{9} \frac{\theta_{i\max} \cdot D_1'(\theta_{i\max}/T) - \theta_{i\min} \cdot D_1'(\theta_{i\min}/T)}{\theta_{i\max} - \theta_{i\min}}\right] + \frac{k_\mathrm{B}N_{at}}{3} \sum_j g_j \cdot \left(\frac{\theta_{ej}}{T}\right)^2 \cdot \frac{\mathrm{e}^{\theta_{ej}/T}}{(\mathrm{e}^{\theta_{ej}/T} - 1)^2}. \tag{12}$$

CTE can be expressed through the bulk elastic modulus B_T and the derivative of pressure over temperature. Assuming that the Grüneisen constants are independent of temperature, one can obtain from (12):

$$\alpha_p = \frac{1}{B_T} \cdot \left(\frac{\partial p}{\partial T}\right)_V = \frac{1}{B_T(T) \cdot V} \cdot \sum_{i=1}^{9} \gamma_{Gi} \cdot C_{V\,i}(V,T) + V \cdot \frac{\partial^2 \langle \varepsilon_{ej} \rangle}{\partial V \,\partial T}, \tag{13}$$

where $C_{Vi}(V,T)$ is the heat capacity of the ith phonon branch. If the Grüneisen constants are the same in all the modes, and the spectrum of electronic excitations does not depend on temperature, then the last expression can be transformed to well-known relationship:

$$\alpha_p(V,T) = \frac{\gamma_G \cdot C_V(V,T)}{B_T(T) \cdot V}. \tag{14}$$

5. Results of calculations and experimental data

In order to be able to use the obtained above formulae for calculation of the AnO_2 thermal properties, the input information about their lattice parameters and the longitudinal and transverse sound velocity v_L and v_T has to be known, which are determined by the Young's (E_s) modulus, the Poisson's ratio (μ) and density (ρ). The recommended values of these parameters at standard temperature and pressure (STP) are presented in Table 1. Unfortunately, we did not found all needed elastic constants, therefore the approximation $\mu \sim 1/3$ has been used when appropriate. The localised electron excitation levels found in literature are presented in Table 2.

5.1. Uranium dioxide

UO_2 case has been analysed first for the model validation. The characteristic temperatures were calculated on the basis of the lattice parameter and elastic constants recommended for the UO_2 monocrystal [4,12]. The temperature dependence of the bulk elastic modulus was taken from [13]. For the TD Grüneisen parameter the value of 1.9 was recommended in [14] as the best estimate. The contribution of different mechanisms to the UO_2 heat capacity is illustrated by Fig. 3. In the considered temperature range of 30 to 2000 K, the normal harmonic vibrations of the lattice play the dominant role. The relative electronic contribution is maximum 5–7% and reduces with temperature at $T > 300$ K. Contrary, the anharmonic contribution related to the lattice expansion increases with temperature and reaches about 20% at $T = 2000$ K. Fig. 4 shows that the calculated heat capacity is in good agreement with the experimental data [16,27,30–32] in the large temperature range from 40 to 2000 K. The agreement between the calculated and recommended [15,27,33] values of the volumetric CTE is less good (Fig. 5). The model underestimates CTE at $T > 1700$ K. It can be due to higher anharmonic or defect contribution.

5.2. Thorium dioxide

The input elastic parameters for ThO_2 were selected from non-exhaustive published data on polycrystalline thorium dioxide [13,16–19]. The same value of the Grunëisen parameter was used (e.g. $\gamma_G = 1.9$). An excellent agreement between the calculated and recommended in [16] values of the specific heat was obtained in the

Table 1
Some parameters of the actinide oxides of interest at STP [9,12,15,18,29]

		ThO_2	UO_2	NpO_2	PuO_2	AmO_2	CmO_2
Molecular mass	g/mol	264.037	270.029	269.047	271.051	275.060	279.062
Lattice parameter	10^{-10} m	5.5968	5.4704	5.425	5.396	5.3772	5.359
Theoretical density	kg/m^3	10002.5	10956.2	11192.8	11458.9	11751.3	12043.6
Young modulus	10^{11} Pa	2.61	2.334	(...)	2.684	(...)	(...)
Poisson's ratio	–	0.28	0.32	(0.333)	0.28	(0.333)	(0.333)
Bulk isothermal modulus	10^{11} Pa	1.98	2.11	2.00	(...)	(200)	(...)

Table 2
Levels of excitation of the localised electrons (in cm^{-1}) [10,11]

	Level	ThO_2	UO_2	NpO_2	PuO_2	AmO_2	CmO_2
k_1	0	–	3×0	2×0	1×0	2×0	–
k_2	1	–	2×1246	4×465.3	3×922.8	4×328	–
k_3	2	–	3×1372	2×2051	3×1776.4	–	–
k_4	3	–	1×1425.5	–	2×2152.5	–	–

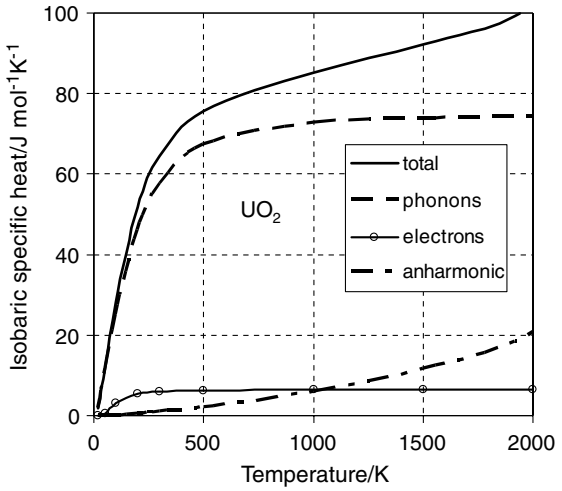

Fig. 3. Contribution of different mechanisms to the heat capacity of UO_2.

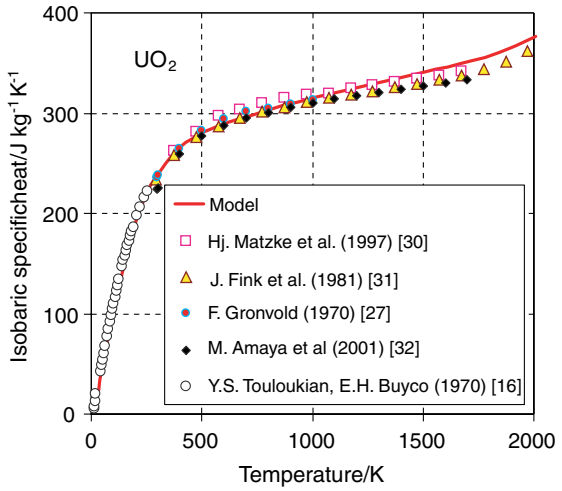

Fig. 4. Calculated and experimental values of the isobaric specific heat of UO_2.

temperature region from 20 to 1800 K. CTE is rather well described by the model at low and middle temperatures (Fig. 6). At low temperatures, the values recommended in [17] are probably not correct because of a very strong deviation from the 'cubic temperature law'. The model overestimates CTE at $T > 1300$ K, and this difference increases almost linearly with temperature. It could be due to the used assumption that the level of anharmonicity (γ_G) in ThO_2 is the same as in UO_2.

5.3. Neptunium dioxide

Most of the input parameters have been taken from the recent publications [20–23]. A rather good agreement between the available experimental data and the results of calculations is demonstrated in Figs. 7 and 8.

5.4. Plutonium dioxide

The room temperature parameters of PuO_2 for the model input were taken from [15]. A satisfactory agreement exists between the calculated and experimental values of the heat capacity at low (30–400 K) [16] and high (>1400 K) [24,34] temperatures (Fig. 9). A disagreement at intermediate temperatures could be due

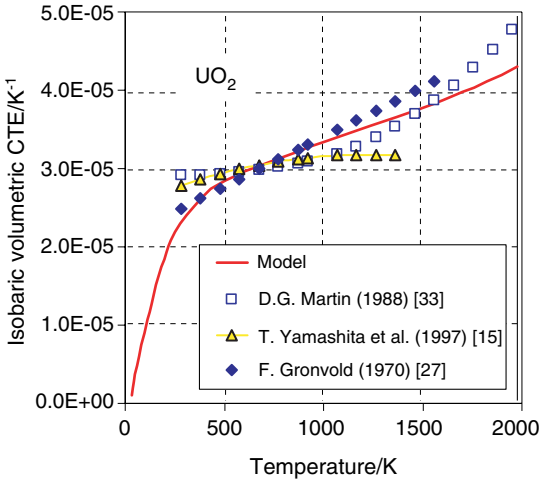

Fig. 5. Calculated and experimental values of the isobaric thermal expansion coefficient of UO_2.

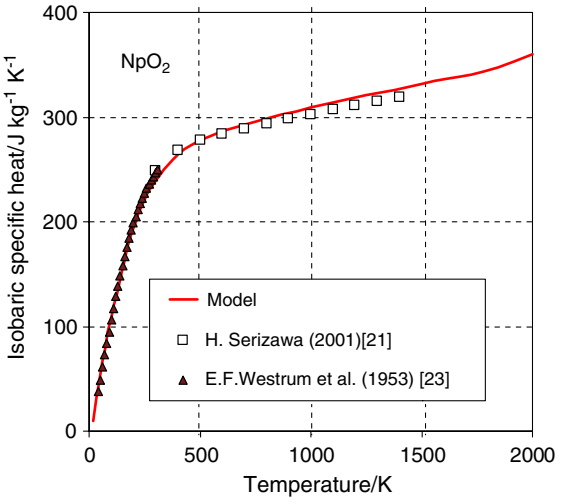

Fig. 7. Calculated and experimental values of the isobaric specific heat of NpO_2.

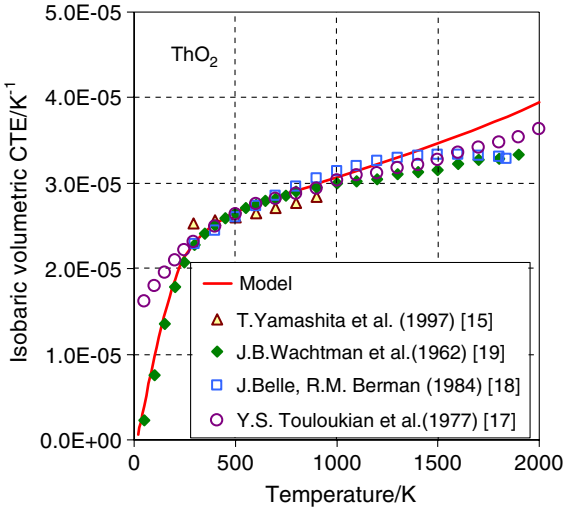

Fig. 6. Calculated and experimental values of the isobaric thermal expansion coefficient of ThO_2.

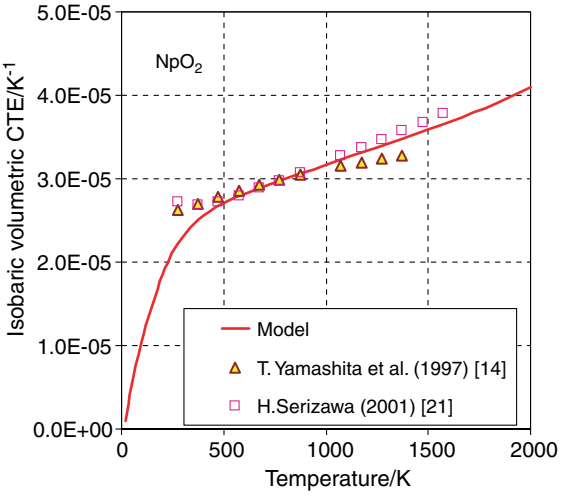

Fig. 8. Calculated and experimental values of the isobaric thermal expansion coefficient of NpO_2.

to a more defective structure of PuO_2 caused by self-irradiation, or due to unknown higher levels of the electron excitations. The satisfactory results were obtained for CTE at temperatures $T > 300$ K (Fig. 10).

5.5. Americium dioxide

The information about AmO_2 mechanical parameters is missing, therefore a value of 200 GPa for the bulk elastic modulus obtained with molecular dynamic modelling was used in the calculations. The calculated heat capacity of AmO_2 was compared with the recommendations of [25,26]. A good agreement was obtained with the results of [25] in the region of 300–1600 K (Fig. 11).

5.6. Curium dioxide

The missing input data for CmO_2, was replaced by those of AmO_2 except the spectrum of electronic excitations (in [25] it was indicated that the electronic

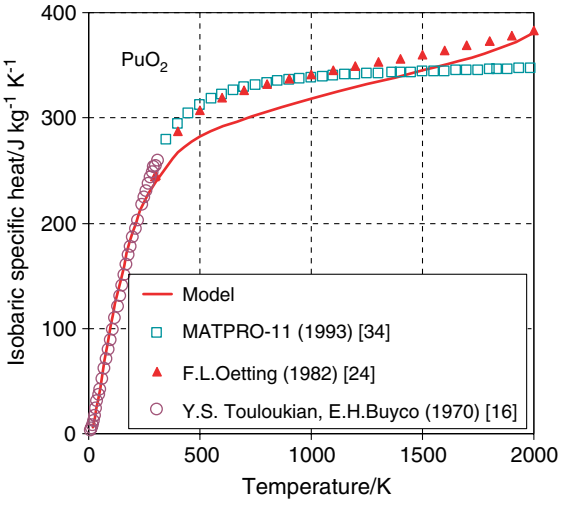

Fig. 9. Calculated and experimental values of the isobaric specific heat of PuO_2.

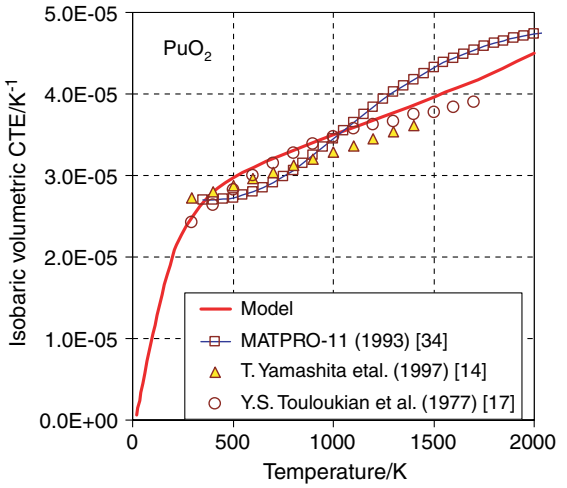

Fig. 10. Calculated and experimental values of the isobaric thermal expansion coefficient of PuO_2.

excitations are absent in CmO_2). The results and recommendations of [11] and [26] are presented in Fig. 11. The model underestimates the CmO_2 heat capacity, indicating to the existence of another (than phonon) contribution. We found only two references with the constant (perhaps mean) values of the linear CTE for americium oxides: $1.016 \times 10^{-6}\ K^{-1}$ in [11] and $8.1 \times 10^{-6}\ K^{-1}$ was cited in [28] but for Cm_2O_3. In the temperature range of 300–650 K, the model yields the mean linear CTE of $0.7 \times 10^{-6}\ K^{-1}$. An increase in the lattice parameter due to self-irradiation defects related to α-decay of curium could be the most probable reason of this disagreement.

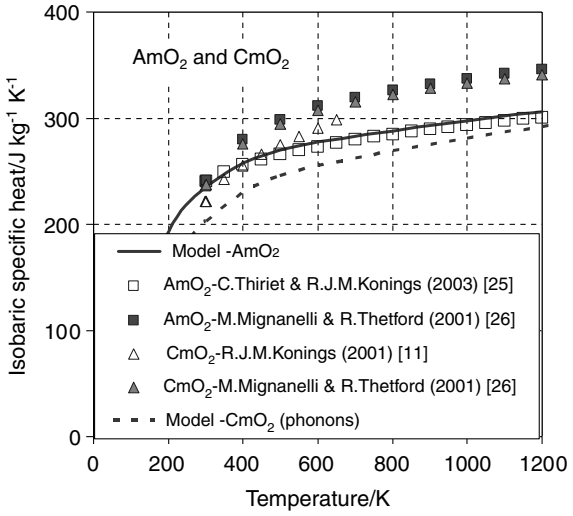

Fig. 11. Calculated and experimental values of the isobaric specific heat of AmO_2 and CmO_2.

6. Conclusions

In the framework of studies of thermal and mechanical performances of oxide fuels with a high content of MA, a simplified model of EOS of actinide dioxides was developed based on a quasi-harmonic approximation for lattice vibrations and a discrete spectrum for electronic excitations. Some improved expressions were deduced allowing to calculate the isochoric and isobaric specific heat and the isobaric coefficient of thermal expansion in a large temperature range. The developed model was validated with the available data on TD properties of UO_2 and ThO_2. Rather good agreement was obtained for the specific heat in the temperature range of 25–1800 K and for the coefficient of thermal expansion in the range of 400–1700 K. The model was also applied for calculation of the heat capacity and the thermal expansion of PuO_2 and minor actinide dioxides: NpO_2, AmO_2, CmO_2. A very good agreement was obtained for NpO_2. Some underestimation of PuO_2 heat capacity in the range of medium temperatures should still be explained. Lack of experimental data on thermal properties of AmO_2 and CmO_2 did not allow a reliable comparison.

The developed methodology can be applied for the prognosis of thermal properties of other forms of nuclear fuel for which the data are still unavailable or incomplete.

Acknowledgement

This work was supported by funds of the MYRRHA project of SCK·CEN and by the FUTURE project of the EURATOM 5th Framework Programme.

References

[1] C.B. Basak, A.K. Sengupta, H.S. Kamath, J. Alloys and Compounds 360 (2003) 210.
[2] K. Kurosaki, K. Yamada, M. Uno, Sh. Yamanaka, K. Yamamoto, T. Namekawa, J. Nucl. Mater. 294 (2001) 160.
[3] P.J.D. Lindan, M.J. Cillanet, J. Phys.: Condensed Matter 3 (1991) 3929.
[4] G. Dolling, R.A. Cowley, A.D.B. Woods, Canadian J. Phys. 43 (1965) 1397.
[5] C. Kittel, Introduction to Sol. State Phys., 2nd Ed., Wiley, New York, 1956.
[6] G.J. Hyland, J. Ralph, High Temp.–High Press. 15 (1983) 191.
[7] M. Kumar, S.S. Bedi, Phys. Stat. Sol. (b) 196 (1996) 303.
[8] G.A. Slack, The Thermal Conductivity of Non-metallic Crystals, in: H. Ehrehrech, F. Scitz, D. Turnbull (Eds.), Solid State Physics, vol. 34, Academic Press, New York, 1979.
[9] R.J.M. Konings, f-MWD Data Base, http://www.f-elements.net/.
[10] J.C. Krupa, Z. Gajek, Eur. J. Solid State Inorg. Chem. 28 (1991) 143.
[11] R.J.M. Konings, J. Nucl. Mater. 298 (2001) 255.
[12] J.B. Wachtman, M.L. Wheat, H.J. Anderson, J.L. Bates, J. Nucl. Mater. 16 (1965) 39.
[13] M. Hoch, J. Nucl. Mater. 130 (1985) 94.
[14] T. Yamashita, N. Nitani, T. Tsuji, T. Kato, J. Nucl. Mater. 247 (1997) 90.
[15] T. Yamashita, N. Nitani, T. Tsuji, H. Inagaki, J. Nucl. Mater. 245 (1997) 72.
[16] Y.S. Touloukian, E.H. Buyco (Eds.), Specific Heat-non-metallic Solids, The TRPC Data Series, Vol. 5., Plenum, New York, 1970.
[17] Y.S. Touloukian, R.K. Kirby, R.E. Taylor, T.Y.R. Lee (Eds.), Thermal Expansion-nonmetallic Solids, The TRPC Data Series, Vol. 13., Plenum, New York, 1977.
[18] J. Belle, R.M. Berman, Thorium Dioxide: Properties and nuclear applications, Naval Reactors Office, USDOE, DOE/NE-0060, 1984.
[19] J.B. Wachman, T.G. Scudert, G.W.J. Cleek, Am. Ceram. Soc. 45 (1962) 319.
[20] H. Serizawa, Y. Arai, J. Alloys Comp. 312 (2000) 257.
[21] H. Serizawa, J. Chem. Thermodynamics 33 (2001) 615.
[22] H. Serizawa, Y. Arai, Y. Suzuki, J. Nucl. Mater. 280 (2000) 99.
[23] E.F. Westrum, J.B. Hatcher, D.W.J. Osborne, Chem. Phys. 21 (1953) 419.
[24] F.L. Oetting, J. Nucl. Mat. 105 (1982) 257.
[25] C. Thiriet, R.J.M. Konings, J. Nucl. Mater. 320 (2003) 292.
[26] M.A. Mignanelli, R. Thetford, in: The Second Workshop Proceedings of the International Conference on Advanced Reactors with Innovative Fuels (ARWIF-2001), Chester, UK, 2001.
[27] F. Grønvold, N.J. Kvetseth, J. Chem. Thermodyn. 2 (1970) 665.
[28] W.C. Mosley, J. Inorg. Nucl. Chem. 34 (1972) 539.
[29] U. Benedict, S. Dabos, C. Dufour, J.C. Spirlet, M. Pagès, J. Less-Common Metals 121 (1986) 461.
[30] Hj. Matzke, P.G. Lucuta, R.A. Verrall, J. Henderson, J. Nucl. Mater. 247 (1997) 121.
[31] J. Fink, M.G. Chasanov, L. Leibowitz, J. Nucl. Mater. 102 (1981) 17.
[32] M. Amaya, K. Une, K. Minato, J. Nucl. Mater. 294 (2001) 1.
[33] D.G. Martin, J. Nucl. Mater. 152 (1988) 94.
[34] MATPRO–A Library of Materials Properties for Light–Water–Reactor Accident Analysis in: SCDAP/RELAP5/MOD3.1 Code Manual, Vol. IV, NUREG/CR-6150 EGG-2720, INEL, USA, 1993.